ISSN 1070-3284, Russian Journal of Coordination Chemistry, 2021, Vol. 47, No. 9, pp. 587–592. © Pleiades Publishing, Ltd., 2021.
Russian Text © The Author(s), 2021, published in Koordinatsionnaya Khimiya, 2021, Vol. 47, No. 9, pp. 529–534.

*Dedicated to Academician N.T. Kuznetsov on the occasion of his 90th birthday*

# Amidophenolate Tantalum Complexes

**P. A. Petrov[a], *, E. A. Golubitskaya[a], I. V. El'tsov[b], T. S. Sukhikh[a], and M. N. Sokolov[a]**

[a] *Nikolaev Institute of Inorganic Chemistry, Siberian Branch, Russian Academy of Sciences, Novosibirsk, Russia*

[b] *Novosibirsk State University, Novosibirsk, Russia*

**e-mail: panah@niic.nsc.ru*

Received March 9, 2021; revised April 16, 2021; accepted April 19, 2021

**Abstract**—Mixed-ligand amidophenolate complexes [Ta($AP^{Dipp}$)($NMe_2$)$_3$] (**I**) and [Ta($AP^{Dipp}$)$_2$($NMe_2$)] (**II**) were obtained by the reaction of Ta($NMe_2$)$_5$ with 2,4-di-*tert*-butyl-6-((2,6-diisopropylphenyl)amino)phenol ($H_2AP^{Dipp}$). The products were characterized by X-ray diffraction (CIF file CCDC nos. 2060699 (**I**), 2060700 (**II**·0.5$C_5H_{12}$)) and NMR spectroscopy.

**Keywords:** tantalum, amines, amidophenolates, X-ray diffraction

**DOI:** 10.1134/S1070328421090074

## INTRODUCTION

Bidentate N-substituted *o*-iminobenzoquinones are structural analogues of *o*-benzoquinones and diimines [1]. These three classes of ligands belong to the type of redox-active ligands, as they can undergo a series of reversible redox transitions (Scheme 1; $IQ^R$ = iminoquinone; $(ISQ^R)^{-\bullet}$ = iminosemiquinolate; $(AP^R)^{2-}$ = amidophenolate). The redox potentials of *o*-iminoquinones are shifted to more negative region in comparison with *o*-quinone potentials. On the other hand, the steric effect of iminobenzoquinones is less pronounced than that for diimines. Thus, the use of iminoquinone derivatives as ligands provides the possibility of steric and electronic tuning of the coordination unit, e.g., for the preparation of complexes with a desired magnetic behavior [2–11]. Furthermore, complexes with iminobenzoquinone derivatives can undergo oxidative addition and reductive elimination reactions, which do not change the oxidation state of the central atom, but affect the π-system of the ligand. These reactions can be either stoichiometric [12–16] or catalytic [17].

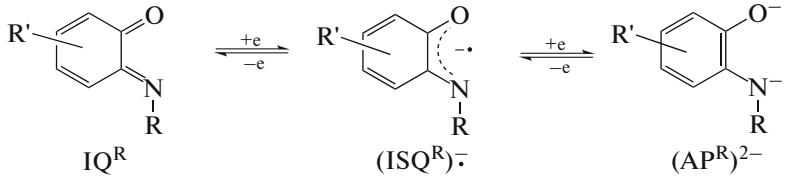


$IQ^R$ $(ISQ^R)^{-\bullet}$ $(AP^R)^{2-}$

**Scheme 1.**

Currently, there are two key methods for the synthesis of catecholate and semiquinolate complexes. The first one is the reaction of quinone with a metal or a low-valent metal complex (most often, carbonyl). In this case, quinone oxidizes a relatively active metal or its compound, being thus reduced to either catecholate or semiquinolate, depending on the reaction conditions. The second method is displacement of the ligand upon the reaction of metal halide with catecholate or semiquinolate (most often, of Na, K, or Tl). In the case of niobium and tantalum, the weak spot of this approach is that niobium and tantalum halides are highly reactive and can, in particular, cleave the C–O bonds of ether solvents [18, 19]. The lack of convenient metal-containing precursors seems to be responsible for the very small number of known niobium and tantalum catecholates. The only currently known catecholate complex of tantalum, [Ta($Cat$)$_2$($HCat$)($Py$)], was obtained by the reaction of Ta($OEt$)$_5$ with catechol at 1 : 3 ratio in pyridine [20]. The niobium complex was prepared in a similar way. On the other hand, amides (in particular, dialkylamides) of early transi-

tion metals are known to be convenient precursors of other compounds.

This study is devoted to the reaction of tantalum(V) dimethylamide $Ta(NMe_2)_5$ with 2,4-di-*tert*-butyl-6-((2,6-diisopropylphenyl)amino)phenol ($H_2AP^{Dipp}$) containing a bulky diisopropylphenyl substituent at nitrogen.

## EXPERIMENTAL

The syntheses were carried out in an inert atmosphere using standard Schlenk technique. The solvents were dehydrated and degassed by refluxing and distillation under argon using appropriate drying agents. The NMR spectra were measured on a Bruker Avance III 500 spectrometer, operating at 500.03 MHz for $^1H$, 125.73 MHz for $^{13}C$, and 50.67 MHz for $^{15}N$, using solvent signals as standards ($\delta(^1H)$ = 7.16 ppm, $\delta(^{13}C)$ = 128.06 ppm) [21]. The $^{15}N$ NMR spectra were obtained as the projection of 2D $^1H,^{15}N$ HMBC correlation; the signals were referred to external formamide standard ($\delta(^{15}N)$ = 112.5 ppm). The structure determination and signal assignment in the $^1H$, $^{13}C$, and $^{15}N$ NMR spectra were carried out using 2D $^1H,^{13}C$ HMBC, $^1H,^{15}N$ HMBC, and $^1H,^{13}C$ HSQC correlations. Elemental analysis was performed at the Analytical Laboratory of the Nikolaev Institute of Inorganic Chemistry, Siberian Branch, Russian Academy of Sciences.

**Synthesis of [Ta(AP$^{Dipp}$)(NMe$_2$)$_3$] (I).** $Ta(NMe_2)_5$ (150 mg, 0.37 mmol) and $H_2AP^{Dipp}$ (145 mg, 0.38 mmol) were placed into a Schlenk vessel and evacuated. Toluene (30 mL) was condensed into the vessel under reduced pressure with liquid nitrogen cooling. After warming up to room temperature, the resulting orange solution was heated on an oil bath ($T$ = 55°C) with stirring for 2 days. The solvent was evaporated in vacuum, the residue was extracted with pentane (30 mL), and the extract was decanted into a double-elbow tube. Slow evaporation resulted in the formation of orange crystals. The yield was 77 mg (30%).

$^1H$ NMR (500 MHz; $C_6D_6$; δ, ppm): 1.15 (d, $J$ = 7.0 Hz, 6H, CH(C$\underline{H}_3$)$_2$), 1.29 (d, $J$ = 7.0 Hz, 6H, CH(C$\underline{H}_3$)$_2$), 1.32 (s, 9H, *t*-Bu-4), 1.74 (s, 9H, *t*-Bu-6), 2.21, 2.69 (br.s, 12H, N(CH$_3$)$_2$), 3.25 (br.m, 14H, N(CH$_3$)$_2$ and C$\underline{H}$(CH$_3$)$_2$), 6.12 (d, $J$ = 2.1 Hz, 1H, CH-3), 7.10 (d, $J$ = 2.1 Hz, 1H, CH-5), 7.17 (t, $J$ = 7.7 Hz, 1H, CH-4 (Dipp)), 7.28 (d, $J$ = 7.7 Hz, 2H, CH-3 (Dipp)).

$^{13}C\{^1H\}$ NMR (126 MHz; $C_6D_6$; δ, ppm): 24.1 (CH(C$\underline{H}_3$)$_2$), 26.5 (CH(C$\underline{H}_3$)$_2$), 28.8 (C$\underline{H}$(CH$_3$)$_2$), 30.5 (C(C$\underline{H}_3$)$_3$(*t*-Bu-6)), 32.3 (C(C$\underline{H}_3$)$_3$(*t*-Bu-4)), 34.7 (C(CH$_3$)$_3$(*t*-Bu-4)), 35.1 (C(CH$_3$)$_3$(*t*-Bu-6)), 39.0 (N(CH$_3$)$_2$), 44.6 (N(CH$_3$)$_2$), 46.7 (N(CH$_3$)$_2$), 110.3 (C-3), 113.4 (C-5), 123.6 (C-3,5 (Dipp)), 126.0 (C-4 (Dipp)), 134.4 (C-6), 139.6 (C-4), 144.7 (C-2,6 (Dipp)), 150.1 (C–O), 150.9 (C–N).

$^{15}N$ NMR (51 MHz; $C_6D_6$; δ, ppm): 211.5 (NDipp).

IR (KBr; ν, cm$^{-1}$): 2961 s, 2867 m, 1653 m, 1636 m, 1558 m, 1541 m, 1472 m, 1457 s, 1437 m, 1419 m, 1361 w, 1326 m, 1240 m, 1102 m, 1026 m, 990 m, 796 m, 743 w, 538 w.

| For $C_{32}H_{55}N_4OTa$ | | | |
|---|---|---|---|
| Anal. calcd., % | C, 55.48 | H, 8.00 | N, 8.09 |
| Found, % | C, 55.10 | H, 7.85 | N, 8.25 |

**Synthesis of [Ta(AP$^{Dipp}$)$_2$(NMe$_2$)]·0.5C$_5$H$_{12}$ (II·0.5C$_5$H$_{12}$).** $Ta(NMe_2)_5$ (100 mg, 0.249 mmol) and $H_2AP^{Dipp}$ (192 mg, 0.503 mmol) were placed into a Schlenk vessel and evacuated. Toluene (30 mL) was condensed into the vessel under reduced pressure with liquid nitrogen cooling. After warming up to room temperature, the resulting orange-red mixture was heated on an oil bath ($T$ = 55°C) with stirring for two days. The solvent was evaporated in vacuum, the residue was extracted with pentane (30 mL), and the extract was decanted into a double-elbow tube. Slow evaporation resulted in the formation of dark red oil, in which bundles of red-brown crystals were formed after careful heating in an air bath for 3 days. The yield was 150 mg (61%).

$^1H$ NMR (500 MHz, $C_6D_6$ δ, ppm): 1.10 (d, $J$ = 6.9 Hz, 6H, CH(C$\underline{H}_3$)$_2$-2), 1.13 (s, 9H, *t*-Bu-4), 1.20 (s, 9H, *t*-Bu-6), 1.22 (d, $J$ = 6.7 Hz, 6H, CH(C$\underline{H}_3$)$_2$-2), 1.30 (d, $J$ = 6.9 Hz, 6H, CH(C$\underline{H}_3$)$_2$-6), 1.40 (d, $J$ = 7.0 Hz, 6H, CH(C$\underline{H}_3$)$_2$-6), 3.39 (s, 6H, N(CH$_3$)$_2$), 3.49 (sept., $J$ = 6.8 Hz, 2H, C$\underline{H}$(CH$_3$)$_2$-2), 3.51 (sept., $J$ = 6.9 Hz, 2H, C$\underline{H}$(CH$_3$)$_2$-6), 6.14 (d, $J$ = 2.1 Hz, 2H, CH-3), 6.92 (d, $J$ = 2.1 Hz, 1H, CH-5), 7.20 (dd, 2H, $^3J$ = 7.6 Hz, $^4J$ = 2.0 Hz, CH-3 (Dipp)), 7.22 (t, 2H, $J$ = 7.6 Hz, CH-4 (Dipp)), 7.32 (dd, 2H, $^3J$ = 7.1 Hz, $^4J$ = 2.0 Hz, CH-5 (Dipp)).

$^{13}C\{^1H\}$ NMR (126 MHz, $C_6D_6$ δ, ppm): 24.7 (CH(C$\underline{H}_3$)$_2$-6), 25.3 ((CH(C$\underline{H}_3$)$_2$)-2), 25.5 ((CH(C$\underline{H}_3$)$_2$)-2), 25.5 ((CH(C$\underline{H}_3$)$_2$)-6), 28.5 ((C$\underline{H}$(CH$_3$)$_2$)-6), 28.6 ((C$\underline{H}$(CH$_3$)$_2$)-2), 30.1 (C(C$\underline{H}_3$)$_3$(*t*-Bu-6)), 31.8 (C(C$\underline{H}_3$)$_3$(*t*-Bu-4)), 34.6 (C(CH$_3$)$_3$(*t*-Bu-6)), 34.8 (C(CH$_3$)$_3$(*t*-Bu-4)), 44.3 (N(CH$_3$)$_2$)), 110.3 (C-3), 114.6 (C-5), 123.7 (C-5 (Dipp)), 125.3 (C-3 (Dipp)), 125.7 (C-4 (Dipp)), 135.6 (C-6), 143.5 (C-1 (Dipp)), 144.3 (C-4), 145.3 (C-6 (Dipp)), 145.7 (C-2 (Dipp)), 146.9 (C–O), 151.6 (C–N).

$^{15}N$ NMR (51 MHz, $C_6D_6$ δ, ppm): 189.7 (NMe$_2$), 206.8 (NDipp).

IR (KBr, ν, cm$^{-1}$): 3057 w, 2963 s, 2867 s, 2790 w, 1576 m, 1465 s, 1442 s, 1410 s, 1360 m, 1321 m, 1286 m, 1251 m, 1229 m, 1201 s, 1109 w, 1056 w,

**Table 1.** Crystallographic data and structure refinement parameters for **I** and **II**·0.5$C_5H_{12}$

| Parameter | Value | |
|---|---|---|
| | **I** | **II**·0.5$C_5H_{12}$ |
| Molecular formula | $C_{32}H_{55}N_4OTa$ | $C_{56.5}H_{86}N_3O_2Ta$ |
| $M$ | 692.75 | 1020.23 |
| System, space group | Triclinic, $P\bar{1}$ | Monoclinic, $P2_1/n$ |
| $a$, Å | 10.1202(5) | 11.3038(6) |
| $b$, Å | 12.1128(7) | 23.2747(13) |
| $c$, Å | 14.6967(8) | 20.7177(11) |
| α, deg | 93.090(2) | 90 |
| β, deg | 98.061(2) | 91.566(2) |
| γ, deg | 110.526(2) | 90 |
| $V$, Å$^3$ | 1660.18(16) | 5448.6(5) |
| $Z$ | 2 | 4 |
| μ, mm$^{-1}$ | 3.339 | 2.058 |
| Crystal size, mm | 0.27 × 0.22 × 0.18 | 0.23 × 0.21 × 0.05 |
| $F$(000) | 712.0 | 2140.0 |
| Data collection range of 2θ, deg | 3.612–54.262 | 2.632–48.812 |
| Range of indices $h$, $k$, $l$ | $-12 \le h \le 11$, $-15 \le k \le 15$, $-18 \le l \le 18$ | $-13 \le h \le 13$, $-27 \le k \le 27$, $-24 \le l \le 19$ |
| Numbers of measured, unique, and observed ($I > 2\sigma(I)$) reflections | 19766, 7305, 7027 | 57326, 8960, 7060 |
| $R_{int}$ | 0.0215 | 0.0727 |
| Number of refined parameters | 359 | 591 |
| GOOF | 1.064 | 1.172 |
| $R_1$, $wR_2$ ($I > 2\sigma(I)$) | 0.0153, 0.0366 | 0.0624, 0.1270 |
| $R_1$, $wR_2$ (all reflections) | 0.0165, 0.0370 | 0.0828, 0.1336 |
| Number of constraints | 0 | 0 |
| $\Delta\rho_{min}/\Delta\rho_{max}$, e Å$^{-3}$ | −0.48/0.41 | −3.63/1.93 |

977 m, 926 m, 907 m, 857 m, 824 s, 801 m, 748 w, 647 m, 586 m, 554 m.

For $C_{54}H_{80}N_3O_2Ta$

| | | | |
|---|---|---|---|
| Anal. calcd., % | C, 65.90 | H, 8.19 | N, 4.27 |
| Found, % | C, 65.50 | H, 8.15 | N, 4.05 |

**X-ray diffraction study**. All measurements were carried out on a Bruker-Nonius X8 APEX four-circle automated diffractometer (CCD array detector, λ = 0.71073 Å, graphite monochromator). The reflection intensities were measured by φ-scanning of narrow (0.5°) frames. The absorption corrections were applied empirically (SADABS) [22]. The structures were solved using the SHELXS [23] and SHELXT [24] program packages and refined in the SHELXL program package [25] in the anisotropic approximation for non-hydrogen atoms using the Olex2 software shell [26]. The hydrogen atoms were located geometrically and refined in the rigid body approximation. The crystallographic characteristics of the complex and X-ray experiment details are presented in Table 1.

The crystallographic data are deposited with the Cambridge Crystallographic Data Centre (CCDC nos. 2060699 (**I**) and 2060700 (**II**·0.5$C_5H_{12}$); http://www. ccdc.cam.ac.uk/conts/retrieving.html).

## RESULTS AND DISCUSSION

The reaction of $Ta(NMe_2)_5$ and aminophenol $H_2AP^{Dipp}$ (1 : 1) in toluene followed by product recrystallization from pentane resulted in the isolation of the amidophenolate complex $[Ta(AP^{Dipp})(NMe_2)_3]$ (**I**, Scheme 2). The product has a distorted trigonal-bipy-

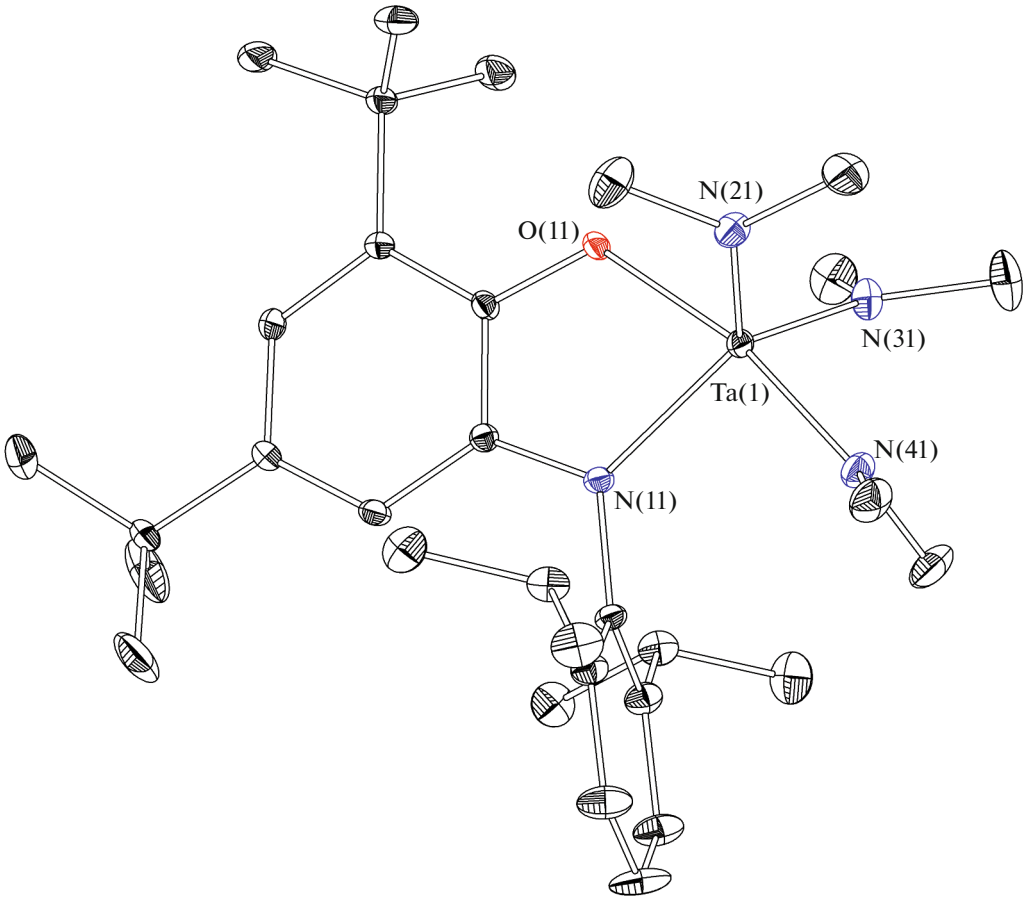


**Fig. 1.** Molecular structure of complex **I**. Selected bond lengths and angles: Ta(1)–O(11), 2.0129(12); Ta(1)–N(11), 2.0632(15); Ta(1)–N(21), 1.9634(15); Ta(1)–N(31), 1.9653(16); Ta(1)–N(41), 1.9958(16) Å; and O(11)Ta(1)N(11), 75.00(5)°.

ramidal structure (Fig. 1), where the N(11), N(21), and N(31) nitrogen atoms form the equatorial plane of the trigonal bipyramid (TBP), with the NTaN angles being 121.51(6)°, 117.27(7)°, and 120.13(6)°. The O(21) and N(41) atoms are in the axial positions, and the Ta(1)–N(41) bond length (1.9959(16) Å) somewhat exceeds the corresponding values for dimethylamide ligands in the equatorial plane of the complex. The quantitative analysis of the structure by Shape program [27, 28] unambiguously attests to TBP as the coordination polyhedron ($S_Q$(TBP) = 0.613).

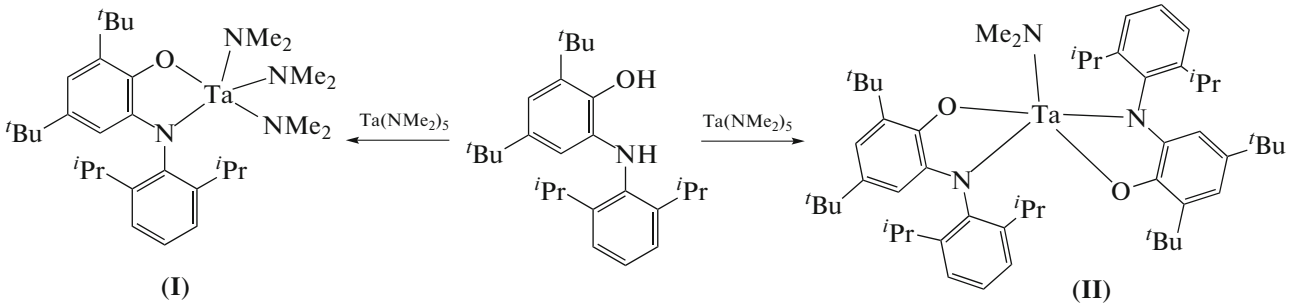


(**I**) (**II**)

**Scheme 2.**

The reaction of $Ta(NMe_2)_5$ with aminophenol $H_2AP^{Dipp}$ in 1 : 2 ratio in toluene followed by recrystallization from pentane resulted in the synthesis of the bis(amidophenolate) complex $[Ta(AP^{Dipp})_2(NMe_2)]\cdot 0.5C_5H_{12}$ (**II**·$0.5C_5H_{12}$). Most likely, complex **II** has a distorted square-pyramidal (CP) structure (Ta

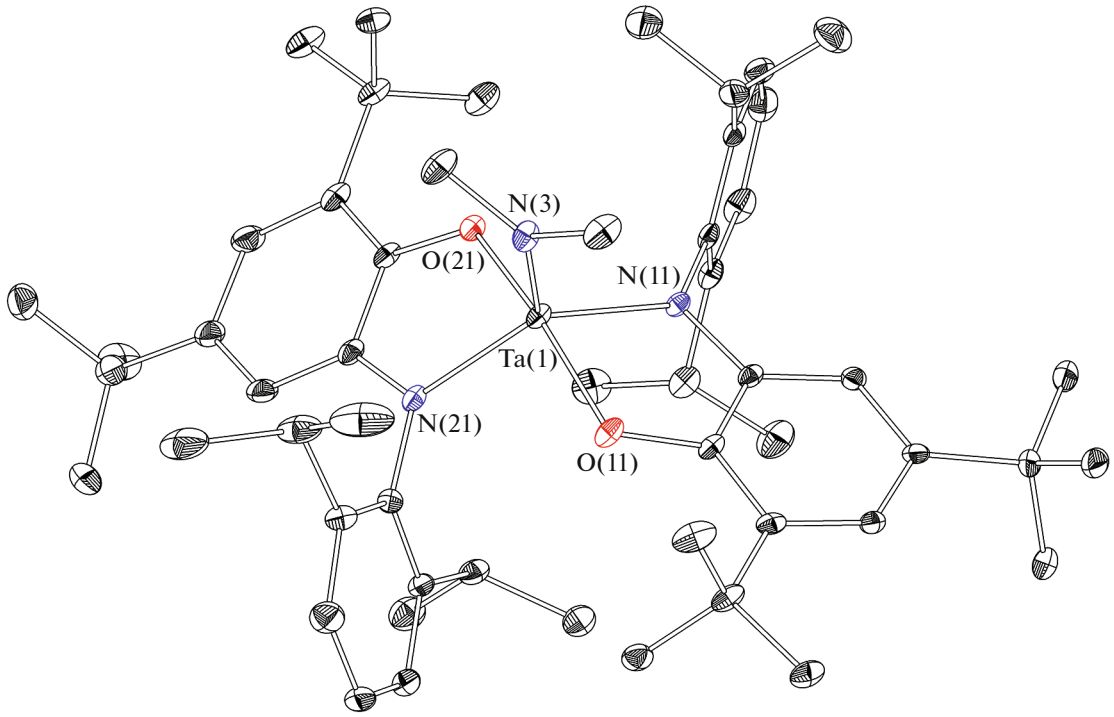


**Fig. 2.** Molecular structure of complex **II**. Selected bond lengths and angles: Ta(1)–O(11), 1.941(5); Ta(1)–O(21), 1.927(5); Ta(1)–N(11), 2.029(7); Ta(1)–N(21), 2.038(7); Ta(1)–N(3), 1.923(7) Å; and O(11)Ta(1)N(11), 78.5(3)°; O(21)Ta(1)N(21), 76.8(3)°.

C.N. = 5), although structure analysis using the Shape program gives comparable values for both (TBP and CP) coordination polyhedra ($S_Q$(TBP) = 1.745, $S_Q$(CP) = 2.115). The amidophenolate ligands are located in the basal plane of the CP in transoid positions relatively to each other (Fig. 2). The C–O and C–N bond lengths of 1.368(10) and 1.417(11) Å are typical of amidophenolates. The Ta(1)–N(3) bond length (1.923(7) Å) and the sum of the three bond angles at N(3) (360.0°) confirm the ligand coordination in the amide form. Alternatively, the coordination polyhedron of complex **II** can be treated as a distorted trigonal bipyramid with three N atoms in the equatorial plane and axial O atoms. The NTaN angles are in the 113.4(3)°–129.8(3)° range, the O(1)Ta(1)O(2) angle is 161.1(2)°, which attests to considerable deviation from the ideal TBP geometry.

The reaction of $Ta(NMe_2)_5$ with $H_2AP^{Dipp}$ in 1 : 3 molar ratio also yields complex **II**. The formation of this product instead of the anionic tris(amidophenolate) $[Ta(AP^{Dipp})_3]^-$ or neutral $[Ta(AP^{Dipp})_2(HAP^{Dipp})]$ is attributable to the presence of bulky diisopropylphenyl substituent at the nitrogen atom. The known homoleptic complexes $[M^{III}(ISQ^R)_3]$ (M = Cr, Fe, Co) contain relatively small phenyl and 3,5-difluorophenyl substituents at the iminosemiquinolate nitrogen [1]. Also, vanadium complex $[V^V(AP^{Ph})_2(HAP^{Ph})]$ containing monoprotonated *N*-phenyl-3,5-di-*tert*-butylamidophenolate is known [1]. This provides the conclusion that that steric restrictions caused by the presence of three bulky diisopropylphenyl groups are too pronounced even for a relatively large central ion such as $Ta^{5+}$.

Complexes **I** and **II** were also characterized by $^1$H, $^{13}$C, and $^{15}$N NMR spectroscopy. The results of analysis indicate a rather rigid conformation of these compounds in solution. The structure of compound **II** is more rigid: for **I**, only the methyl groups of the isopropyl moiety are non-equivalent, whereas in the spectra of **II**, all groups of atoms give rise to separate well-resolved signals. The chemical shifts for arylamide nitrogen virtually coincide for **I** and **II** ($\delta_N$ = 211.5 and 206.8 ppm, respectively). The signal for the dimethylamine ligand in **II** ($\delta_N$ = 189.8 ppm) is somewhat shifted downfield compared to that in $Ta(NMe_2)_5$ (164.6 ppm). In the $^{15}$N NMR spectrum of complex **I**, no signals for dimethylamide ligands were detected, which may be due to insufficiently fast (on the NMR time scale) conformation exchange between the non-equivalent positions of the stereochemically non-rigid structure with C.N. of 5. This assumption is supported by considerable broadening of the $^1$H NMR signals of $NMe_2^-$ groups in complex **I** ($\omega_{1/2}$ ~ 7–25 Hz) in comparison with **II** ($\omega_{1/2}$ ~2 Hz). The carbon signal at the C–N bond (C-2) is shifted upfield in comparison with that of the C–O carbon (C-1). Also, the signal of the

H-3 atom is located in markedly lower field. This is most likely due to the mutually perpendicular positions of the rings: the C-2 carbon atom is located virtually in the plane of the ring of the diisopropylphenyl moiety and experiences the de-shielding effect of the aromatic ring, whereas the H-5 hydrogen atom is located above the ring plane and falls into the shielding region (cf. [29]).

Thus, we demonstrated that the reaction of $Ta(NMe_2)_5$ with aminophenol $H_2AP^{Dipp}$ gives, depending on the reactant ratio, $[Ta(AP^{Dipp})(NMe_2)_3]$ or $[Ta(AP^{Dipp})_2(NMe_2)]$, which represent the first amidophenolate tantalum complexes. The tris-amidophenolate complex cannot be obtained, probably for steric reasons. It is noteworthy that the coordination number for both complexes is five, which suggests a certain coordinative unsaturation and Lewis acidity of the amidophenolate complexes. Complex **II** has a markedly distorted structure intermediate between the CP and TBP geometry of the coordination polyhedron of tantalum.

## CONFLICT OF INTEREST

The authors declare that they have no conflicts of interest.

## REFERENCES


1. Poddel'sky, A.I., Cherkasov, V.K., and Abakumov, G.A., *Coord. Chem. Rev.*, 2009, vol. 253, p. 291.
2. Ershova, I.V., Piskunov, A.V., and Cherkasov, V.K., *Russ. Chem. Rev.*, 2020, vol. 89, p. 1157. https://doi.org/10.1070/RCR4957
3. Ershova, I.V. and Piskunov, A.V., *Russ. J. Coord. Chem.*, 2020, vol. 46, p. 154. https://doi.org/10.1134/S1070328420030021
4. Piskunov, A.V., Pashanova, K.I., Bogomyakov, A.S., et al., *Polyhedron*, 2020, vol. 186, p. 114610.
5. Piskunov, A.V., Meshcheryakova, I.N., Piskunova, M.S., et al., *J. Mol. Struct.*, 2019, vol. 1195, p. 417.
6. Ershova, I.V., Bogomyakov, A.S., Fukin, G.K., and Piskunov, A.V., *Eur. J. Inorg. Chem.*, 2019, p. 938.
7. Chegerev, M.G. and Piskunov, A.V., *Russ. J. Coord. Chem.*, 2018, vol. 44, p. 258. https://doi.org/10.1134/S1070328418040036
8. Piskunov, A.V., Maleeva, A.V., Fukin, G.K., et al., *Inorg. Chim. Acta*, 2017, vol. 455, p. 13.
9. Piskunov, A.V., Ershova, I.V., Bogomyakov, A.S., et al., *Inorg. Chem.*, 2015, vol. 54, p. 6090.
10. Piskunov, A.V., Maleeva, A.V., Bogomyakov, A.S., et al., *Polyhedron*, 2015, vol. 102, p. 715.
11. Piskunov, A.V., Meshcheryakova, I.N., Maleeva, A.V., et al., *Eur. J. Inorg. Chem.*, 2014, p. 3252. https://doi.org/10.1002/ejic.201402116
12. Piskunov, A.V., Meshcheryakova, I.N., Fukin, G.K., et al., *Dalton Trans.*, 2013, vol. 42, p. 10533.
13. Piskunov, A.V., Piskunova, M.S., and Chegerev, M.G., *Russ. Chem. Bull.*, 2014, vol. 63, p. 912.
14. Piskunov, A.V., Ershova, I.V., Fukin, G.K., and Shavyrin, A.S., *Inorg. Chem.* Commun., 2013, vol. 38, p. 1270.
15. Piskunov, A.V., Chegerev, M.G., and Fukin, G.K., *J. Organomet. Chem.*, 2016, vol. 803, p. 51.
16. Matson, E.M., Opperwall, S.R., Fanwick, P.E., and Bart, S.C., *Inorg. Chem.*, 2013, vol. 52, p. 7295.
17. Blackmore, K.J., Lal, N., Ziller, J.W., and Heyduk, A.F., *J. Am. Chem. Soc.*, 2008, vol. 130, p. 2728.
18. Bini, R., Chiappe, C., Marchetti, F., et al., *Inorg. Chem.*, 2010, vol. 49, p. 339.
19. Marchetti, F., Pampaloni, G., and Zacchini, S., *Inorg. Chem.*, 2008, vol. 47, p. 365.
20. Boyle, T.J., Tribby, L.J., Alam, T.M., et al., *Polyhedron*, 2005, vol. 24, p. 1143.
21. Fulmer, G.R., Miller, A.J.M., Sherden, N.H., et al., *Organometallics*, 2010, vol. 29, p. 2176.
22. APEX2 (version 1.08), SAINT (version 7.03), SADABS (version 2.11), SHELXTL (version 6.12), Madison: Bruker AXS Inc., 2004.
23. Sheldrick, G.M., *Acta Crystallogr., Sect. A: Found. Crystallogr.*, 2008, vol. 64, p. 112.
24. Sheldrick, G.M., *Acta Crystallogr., Sect. A: Found. Adv.*, 2015, vol. 71, p. 3.
25. Sheldrick, G.M., *Acta Crystallogr., Sect. C: Struct. Chem.*, 2015, vol. 71, p. 3.
26. Dolomanov, O.V., Bourhis, L.J., Gildea, R.J., et al., *J. Appl. Crystallogr.*, 2009, vol. 42, p. 339.
27. SHAPE (version 2.1), Barcelona: Universitat de Barcelona, 2013.
28. Alvarez, S., Alemany, P., Casanova, D., et al., *Coord. Chem. Rev.*, 2005, vol. 249, p. 1693.
29. Shuvalov, V.Y., Eltsov, I.V., Tumanov, N.A., et al., *Eur. J. Org. Chem.*, 2017, vol. 36, p. 5410.


*Translated by Z. Svitanko*